INTERFACE

rsif.royalsocietypublishing.org

Research

Cite this article: Schnepf A, Leitner D, Schweiger PF, Scholl P, Jansa J. 2016 L-System model for the growth of arbuscular mycorrhizal fungi, both within and outside of their host roots. *J. R. Soc. Interface* **13**: 20160129.
http://dx.doi.org/10.1098/rsif.2016.0129

Received: 13 February 2016
Accepted: 30 March 2016

Subject Category:
Life Sciences–Mathematics interface

Subject Areas:
biomathematics, computational biology

Keywords:
arbuscular mycorrhiza, external hyphae, L-system, mathematical model, root architecture, root system infection

Author for correspondence:
A. Schnepf
e-mail: a.schnepf@fz-juelich.de

Electronic supplementary material is available at http://dx.doi.org/10.1098/rsif.2016.0129 or via http://rsif.royalsocietypublishing.org.

THE ROYAL SOCIETY PUBLISHING

L-System model for the growth of arbuscular mycorrhizal fungi, both within and outside of their host roots

A. Schnepf[1], D. Leitner[2], P. F. Schweiger[3], P. Scholl[4] and J. Jansa[5]

[1]Forschungszentrum Juelich GmbH, Institute of Bio- and Geosciences, IBG-3: Agrosphere, 52425 Juelich, Germany
[2]Computational Science Center, University of Vienna, Oskar Morgenstern-Platz 1, 1090 Vienna, Austria
[3]Department of Microbiology and Ecosystem Science, University of Vienna, Althanstrasse 14, 1090 Vienna, Austria
[4]Institute of Hydraulics and Rural Water Management, BOKU-University of Natural Resources and Life Sciences, Muthgasse 18, 1190 Vienna, Austria
[5]Laboratory of Fungal Biology, Institute of Microbiology, Academy of Sciences of the Czech Republic, Vídeňská 1083, Praha 4 - Krč, 142 20, Czech Republic

AS, 0000-0003-2203-4466

Development of arbuscular mycorrhizal fungal colonization of roots and the surrounding soil is the central process of mycorrhizal symbiosis, important for ecosystem functioning and commercial inoculum applications. To improve mechanistic understanding of this highly spatially and temporarily dynamic process, we developed a three-dimensional model taking into account growth of the roots and hyphae. It is for the first time that infection within the root system is simulated dynamically and in a spatially resolved way. Comparison between data measured in a calibration experiment and simulated results showed a good fit. Our simulations showed that the position of the fungal inoculum affects the sensitivity of hyphal growth parameters. Variation in speed of secondary infection and hyphal lifetime had a different effect on root infection and hyphal length, respectively, depending on whether the inoculum was concentrated or dispersed. For other parameters (branching rate, distance between entry points), the relative effect was the same independent of inoculum placement. The model also indicated that maximum root colonization levels well below 100%, often observed experimentally, may be a result of differential spread of roots and hyphae, besides intrinsic plant control, particularly upon localized placement of inoculum and slow secondary infection.

1. Introduction

Arbuscular mycorrhiza (AM) is an ancient relationship between soil fungi and the majority of land plant species. It is considered to be the most widespread interkingdom symbiosis on Earth. The fungi are obligate biotrophs, completely dependent on the carbon supply from the host plant for their life and reproduction. Through establishment of extensive hyphal networks in the soil, the fungi efficiently gather poorly mobile soil nutrients such as phosphorus and zinc, which they trade for carbon with the host plant [1]. Most often, the extent of root colonization by AM fungi is assessed as the fraction of root length colonized by mycorrhizal hyphae, arbuscules or other structures. A positive relationship between the extent of root colonization and mycorrhizal contribution to plant growth has been demonstrated across a number of glasshouse and field trials ([2] and references therein), although other factors such as the identity of the symbiotic partners obviously contribute another large share of the variability [3–7]. On the other hand, when environmental conditions change, the colonization levels of the roots also often change, indicating a dynamic regulation of the size of the symbiotic interface [8–10]. But so far, the mechanisms behind the regulation of symbiotic interface establishment have not been characterized.

When root and hyphal surfaces meet, a so-called appressorium is formed, and the fungus starts penetrating the cortical cells via a tunnel-like structure [11]. Following the breach through the first layer of root cells (rhizodermis), the fungus spreads within the cortical layer longitudinally along the root. This is where the root and fungal membranes come into very close contact, allowing the exchange of nutrients for carbon. Using the hyphal connection through the appressorium, the fungus develops a branched external hyphal network in the soil, which serves for gathering soil resources as well as infecting other parts of the root system of the same or a neighbouring plant [12]. Patterns of root and soil colonization are among the most important mycorrhizal traits related to plant nutrient acquisition [13]. However, dynamic three-dimensional observations of root system and soil colonization by mycorrhizal fungi are scarce [14,15].

Mathematical modelling has played a significant role in the development of our understanding of the growth and function of the fungal mycelium [16]. For filamentous fungi, two main groups of modelling approaches have been used. The first group involves continuous models based on differential equations. These models are efficient in modelling dense mycelia in homogeneous environments [17]. The second group of models involves discrete models that are based on growth rules for hyphal segments. A model that scales from the growth patterns of individual hyphae to colony dynamics was presented by [18]. Models of hyphal networks were reviewed by [19]. Growth of AM fungi is similar to the growth of other filamentous fungi in that it shows similar processes such as branching, elongation or anastomosis. The major difference to the other (e.g. saprotrophic) fungi is that they are obligate symbionts associated with plant roots. Mutualism between plants and their root symbionts has been studied by non-spatially explicit models, e.g. ecological models [20–22], or by models similar to logistic growth models [23,24]. A spatially explicit model on the single root scale was developed by [25,26].

To improve the mechanistic understanding of the root colonization process by AM fungi, we developed a spatially explicit and dynamic three-dimensional model that predicts root and soil colonization in a growing root system. Thereby, we accurately describe functional traits and processes playing a role in root colonization by AM fungi. We use a new L-system model based on the dynamic, three-dimensional root architecture model described earlier [27] with newly included root system infection with AM fungi and growth of external mycelium. Lindenmayer (L-)systems are rewriting systems based on strings that are interpreted based on a 'turtle geometry', where a point is moved relative to its own position by different commands represented by the strings. This approach is well suited to model branching structures such as root systems that possess a high degree of (topological) self-similarity [28].

In contrast to earlier efforts of modelling mycorrhizas, which all generally described observed patterns by employing a correlative approach, the strength of the presented mycorrhiza model is that it is a numerical simulation, which is to be only ex-post aligned with the experimental data. As such, it allows dissecting the contribution of the different factors to root colonization by the AM fungi.

Potential applications of our model are the simulation of spread of AM fungal infection depending on the localization of infective propagules. Both modelling as well as experimental work show that root colonization changes based on external or internal factors [29], but spatially explicit information is mostly missing. Our model will help to quantify the role of the complex geometrical structure of external mycelia in plant phosphate (P) acquisition and to gain mechanistic insights into whole-plant processes affected by mycorrhizal symbiosis.

2. Model description

The goal of this work was to model the development of AM fungi both in and outside of a growing root system. First, we describe available data and knowledge that was the basis for model development. Parametrization was based on literature data and simulation outcomes were compared with a validation experiment. Subsequently, different hypotheses about the effect of inoculum position and about root system infection mechanisms were tested in several simulation case studies.

2.1. Available data used for model development

Most analyses of mycorrhizal colonization of roots and soil report on the percentage of root length infected by the fungi, hyphal length density of external mycelium, number of entry points per unit root length and P content in the shoot and roots of the host plant [30,31]. Isotope labelling enabled determination of the origin of the P found in the shoot [3,32] and analysis of the external hyphal spread through the soil [7].

A lot of information about the three-dimensional development of mycorrhizal infection inside a growing root system comes from a series of papers in *New Phytologist* 'The development of endomycorrhizal root systems: I–VIII', which were produced from 1977 through 1993 [14,23,24,30,33–36]. At this time, there was much interest in the possibility of inoculation of field crops with selected strains of AM fungi that were more effective promotors of host growth than those indigenous to field soils [30]. In short-season crops, in particular, a significant effect on plant growth may depend on early infection [33], and thus rapidity of infection was regarded as one of the important traits for successful inoculation of plants with AM fungi.

2.2. Model development

The starting point for model development is a dynamic, three-dimensional root architecture model based on L-systems. In the model of Leitner *et al*. [27], a root system is composed of connected segments. We further developed it to include the possibility that each root segment can become infected by mycorrhizal fungi and by considering growth of external fungal hyphae from each infected root segment. We describe the infection of growing roots by mycorrhizal fungi by two distinct processes: first, we assume that there is an average probability for primary infection of root segments caused by fungal propagules present in the soil. Second, we assume that the infection of a new root segment immediately adjacent to an infected segment occurs via secondary infection caused by external hyphae from adjacent infected root segments, with a probability that is much higher than that of primary infection from inoculum.

2.2.1. Primary infection

Depending on the density of the propagules (spores, infected roots) in the soil, root segments can become infected with AM fungi with a certain probability P. To obtain independence from the spatial and temporal resolution, P describes the probability of infection of 1 cm root within 1 day. The probability p

that a root segment of length dx becomes infected over a time period of dt is then given by

$$p = 1 - (1 - P)^{\mathrm{d}t \cdot \mathrm{d}x},$$

where $(1 - P)$ is the probability of 1 cm root not being infected within a day, and $(1 - P)^{\mathrm{d}t \cdot \mathrm{d}x}$ is the probability of not being infected over a time period of dt with a segment length dx.

Infection can occur everywhere but is more likely near the root apex [14]. We assume a so-called susceptible phase of root development, i.e. that there is a maximal root age *maxAge* until which the root can become infected. We also provide the possibility to set a minimum age for infection, *minAge*, but set it equal to zero in all our simulations. We assume the probability of infection is linearly decreasing with the age of the root segment *age* and with p being the maximal possible probability. Therefore, the actual probability p_a of infection is given by the equation

$$p_a = \left(1 - \frac{age}{maxAge}\right) p.$$

Furthermore, the probability P can be spatially heterogeneous, i.e. $P := P(x)$ to describe heterogeneous soil conditions, or experimental scenarios where the inoculum is placed at certain positions.

Based on current absence of evidence for formation of new hyphal connections between internal and external hyphae [37], we operationally assume that already infected segments cannot become infected again and that every infected segment represents one entry point from which external hyphae also start to grow outward into the soil. It is likely that root segments can become re-infected, but this is not experimentally observable and therefore, we follow the approach of Buwalda *et al*. [14] to deal only with observable infections.

2.2.2. Secondary infection

Secondary infection is caused by external hyphae that regularly produce new entry points and thus create new root infections. Neighbouring root segments are most likely candidates for this new infection. Therefore, secondary infection is often viewed as advancing infection fronts inside the roots [34]. In the model, we assume that the chance that a root segment neighbouring an already infected segment itself becomes infected is 100%. We describe this internal infection front advancing along the roots both towards the tip and the base of the root at a constant speed v_i. If the length of the root segment is l, the number of neighbouring segments becoming infected within one time step is therefore equal to round(v_i dt/l).

A maximum percentage *maxInfection* of root length infected by primary and secondary infection can be freely chosen, depending on the fungus–host combination [36]. Primary and secondary infections are only possible if this percentage is not reached.

For simplicity, we do not model the growth of internal fungal hyphae to form so-called infection units [38]. We assume that one root segment is either infected or not infected (ignoring potential dynamics inside this root segment) and each infected root segment hosts one entry point. Therefore, it is convenient to choose the length of one root segment to be equal to the distance between two entry points, e.g. 0.5 mm as quoted by Amijee *et al*. [34].

2.2.3. Growth of external hyphae in soil

The growth of external fungal hyphae in soil is implemented in a similar manner to the growth of roots. We assume that external hyphae have a constant radius a_h and grow with a constant speed v. External fungal hyphae show two additional branching patterns that are not found in root systems: first, fungi can branch dichotomously. The time period between dichotomous branching is $1/b$, where b is the branching rate. The hyphal tip splits into two new tips, and the two external hyphae continue to grow with a branching angle θ_h between them. Second, there is fusion between two hyphal tips (tip–tip anastomosis), and fusion between a hyphal tip and a hypha (tip–hyphae anastomosis). We assume that anastomosis will happen, if the two tips or tip and hyphae come very close to each other. Tip–tip anastomosis is applied if the intertip distance is below a threshold *distTT*. In this case, the tips are connected by an edge and the tips stop growing. Tip–hyphae anastomosis is applied if the distance between tip and hyphae is below the threshold *distTH*. The tip is connected to the mid of the hyphal segment and the tip stops growing. Hyphal death is implemented into the model via the parameter hyphal lifetime (*hlt*) that represents that maximum age of a fungal branch.

2.3. Implementation

The model was implemented by extending the L-system model for root growth, RootBox [27]. It is written in MATLAB® (v. 8.4.0.150421 (R2014b), The MathWorks Inc., Natick, MA) and can be obtained at http://www.csc.univie.ac.at/index.php?page=myc. Root growth and infection are alternately computed at each time step which was set to be 1 day. Each root segment is then flagged as either infected or not infected. Note that the root segment length dx is a user-supplied parameter in the RootBox model. For mycorrhization studies, we suggest that the root segment length is chosen equal to the length of one infection unit. At each time step dt, new root segments may become infected through primary infection or through secondary infection. As soon as a root segment becomes infected, we assume that there is a connection of the infected segment to the soil hyphae through the hyphal trunk being linked to the appressorium, from which one branch starts growing outward into the soil. The appressorium is assumed to be located at mid-point of the infected segment. After each hyphal growth step, we tested whether the conditions for anastomosis were present.

3. Parametrization

3.1. Root system parameters

The root growth part of the model was parametrized for *Medicago truncatula* because this plant species was also used in the validation experiment described below. Root architectural parameters were directly measured by analysing a total of seven previously published [39] images of root systems of *M. truncatula* with ages ranging from 14 to 18 days, with the software 'RootSystemAnalyzer' [40] (exemplarily shown for one 14-day-old root system in figure 1). It provides the parameters required for the RootBox model [41] from two-dimensional images.

Original images were kindly made available to us by V. Bourion. In order to calibrate the root growth model to the root lengths measured in our own experiment, we additionally calibrated three out the 29 root growth parameters (initial elongation rates of tap root and first-order laterals as well as

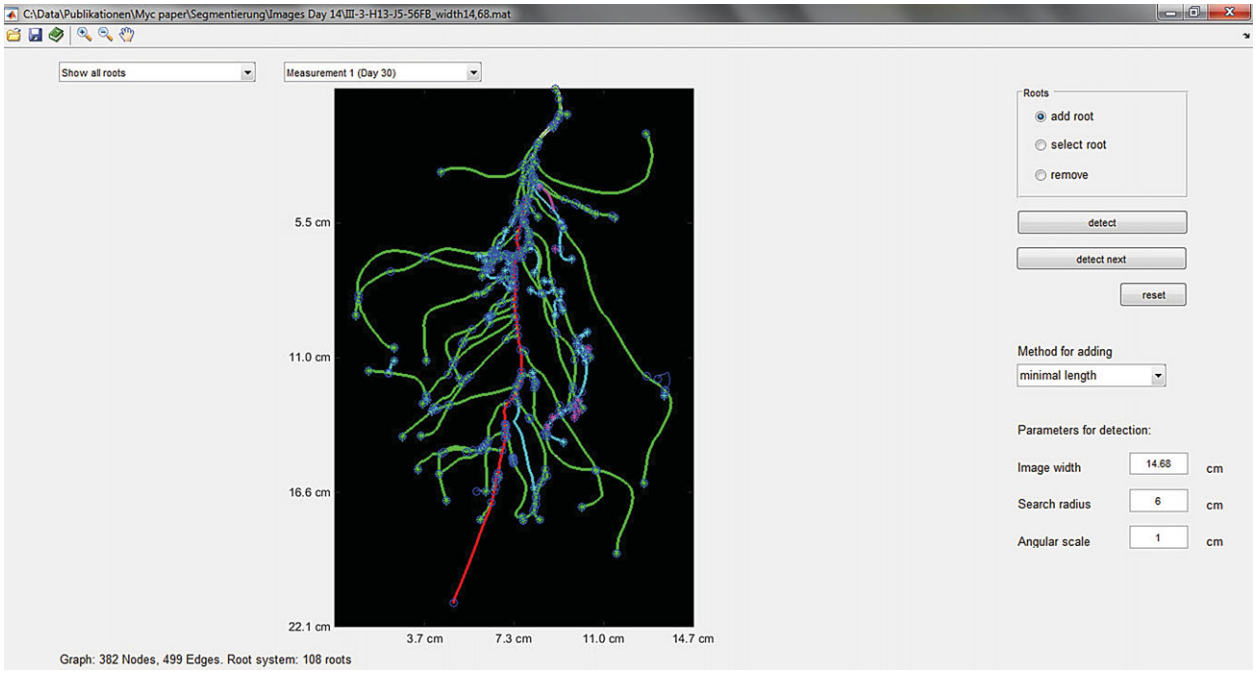

Figure 1. Root tracking in a two-dimensional image of a 14-day-old *Medicago truncatula* plant with RootSystemAnalyzer. The different colours of the roots represent their order (red, tap root; green, first-order lateral; cyan, second-order lateral; magenta, third-order lateral).

maximum number of branches of first-order laterals) to the root length measured in the calibration experiment described below. Resulting root architecture parameter values for the RootBox model are shown in table 1.

3.2. Mycorrhiza model parameters

Mycorrhizal infection in a growing root system was mainly parametrized based on the literature, including different host–fungus combinations. They are the only data of this kind available and we regard the values derived from them as plausible for our simulations. Parameters are given in table 2. Although we implemented the possibility of anastomosis in our model, it is difficult to parametrize because it is also very difficult to observe, particularly in the soil matrix. In addition, it increases the computational time and costs substantially. We therefore deactivated anastomosis for all the following simulations; thus the calculated hyphal length densities should be regarded as an upper limit of the hyphal length density.

4. Calibration experiment

We studied the development of AM root colonization of *M. truncatula* using a two-stage experimental set-up. The aim was to measure the AM colonization rate of a root system connecting to an already established AM soil mycelium. In the first stage, donor plants were grown in 9 l boxes filled with a 10/45/45 (w/w/w) mixture of a moderately low P soil (for soil characteristics, see table 3), coarse sand and zeolite. Half of the boxes received a soil inoculum containing viable propagules of the AM fungus *Rhizophagus irregularis* BEG 158. Control (mock) inoculum with no viable AM propagules was added to the other boxes (non-mycorrhizal control treatment). Each box contained four unplanted root-exclusion bags made of plastic pots of the form of pyramid stumps with a quadratic cross section with 6.3 cm side length at the bottom, 8 cm side length at the top and a depth of 8 cm. Its sides had been removed and replaced with 25 µm nylon meshes. The meshpots contained 525 g of a 50/50 (w/w) mixture of coarse sand and the above soil. For the first (donor) stage of the experiment, surface-sterilized (conc. H_2SO_4 for 10 min) seeds of *M. truncatula* were sown in the boxes around the meshpots and each received 1 ml of a dense suspension of *Sinorhizobium meliloti* (isolate no. 1021; greater than 10^8 cells ml^{-1}). Ten weeks after the start of the donor stage, the meshpots were removed from the boxes and placed into plastic pots of the same size. For the second stage, one two-week-old *M. truncatula* seedling that had been pregrown in sterilized sand was planted into each meshpot and inoculated with a dense *S. meliloti* suspension as above. Owing to poor plant growth, 10.5 mg mineral nitrogen (N) in the form of NH_4NO_3 was added to each pot at 42 days after planting. Plant growth (shoot and root dry weight) was determined at four harvest dates: 36, 50, 64 and 85 days after planting.

The extent of AM root colonization was determined under a compound microscope at 100 times magnification [46] on cleared (10% KOH) and subsequently stained roots (ink and vinegar method; [47]). The abundance of *R. irregularis* hyphal biomass was assessed by real-time PCR including internal DNA standard quantification to correct for different DNA extraction efficiency from the soil samples [48,49]. These data were converted to hyphal length using a conversion factor based on previous experiments with the same fungus of 44 000 000 of mitochondrial large ribosomal subunit gene copies (determined with mt5 molecular marker, J. Jansa 2016, personal communication) per metre of AM fungal hyphae. No appreciable development of the AM fungus was detected in the non-mycorrhizal control treatment. Measured root infection as well hyphal length densities were used to further calibrate the model for the values of the initial position of the inoculum in the containers. Hyphal growth parameters (speed of secondary infection, distance between entry points, elongation rate, branching rate and hyphal lifetime) were taken from the literature. For these parameters, a sensitivity analysis with values representing the literature range of possible parameter values was performed.

Table 1. Root architectural parameters of *Medicago truncatula*.

symbol	parameter name	units	value [mean, s.d.]
tap root			
r	initial tip elongation rate	cm d^{-1}	[2.83, 0]
a	root radius	cm	[0.03, 0.003]
la	length of apical zone	cm	[4.33, 4.61]
lb	length of basal zone	cm	[0.26, 0.24]
ln	internodal distance	cm	[0.26, 0.24]
nob	maximal number of branches	–	178
σ	expected change of root tip heading	rad cm^{-1}	0.20
type	type of tropism	—	1
N	strength of tropism	—	1.5
d*x*	spatial resolution along root axis	cm	0.05
first-order laterals			
r	initial tip elongation rate	cm d^{-1}	[0.98, 0.29]
a	root radius	cm	[0.02, 0.01]
θ	insertion angle	rad	[1.41, 0]
la	length of apical zone	cm	[1.63, 1.69]
lb	length of basal zone	cm	[1.04, 1.24]
ln	internodal distance	cm	[0.82, 1.53]
nob	maximal number of branches	–	2
σ	expected change of root tip heading	rad cm^{-1}	0.30
type	type of tropism	—	1
N	strength of tropism	—	1
d*x*	spatial resolution along root axis	cm	0.05
second-order laterals			
r	initial tip elongation rate	cm d^{-1}	[1.54, 0.28]
a	root radius	cm	[0.01, 0.004]
θ	insertion angle	rad	[1.48, 0]
K	maximal root length	cm	[0.59, 0.78]
σ	expected change of root tip heading	rad cm^{-1}	0.4
type	type of tropism	—	1
N	strength of tropism	—	0
d*x*	spatial resolution along root axis	cm	0.05

5. Sensitivity analysis

Based on the model parameters given in tables 1 and 2, we used the model to perform a sensitivity analysis with freely growing *M. truncatula* root systems. Two cases for the position of AM fungal inoculum in soil were considered. The first scenario (dispersed), inoculum was assumed to be dispersed everywhere in the soil with low probability of infection. This resembles the situation in an agricultural field. In the second scenario (concentrated), no inoculum was dispersed in the entire soil volume, but it was restricted to a small seeding zone with high inoculum density. We assumed a cube of $5 \times 5 \times 5$ cm, with the seed at the centre of the top face of this cube, where the infection probability was 100%, i.e. $p = 1$ inside this small zone and $p = 0$ elsewhere. This would be an extreme situation of an agricultural production system with disinfected soil (e.g. vegetable glasshouse), where the soil does not contain any inoculum but crop growth is supported by the placement of AM fungal inoculum near the seed. Parameter values of the speed of secondary infection, the distance between entry points, the hyphal elongation rate, the hyphal branching rate and the hyphal lifetime were varied one at a time within the range of possible values based on the literature, and their effect on root colonization or external hyphal length densities was assessed. To consider the stochastic nature of the root growth model, all simulations of the sensitivity analysis were based on a sample size of 100 realizations of the root system.

6. Results

6.1. Model calibration with experimental results

Differences in plant dry weight between the mycorrhizal (AM) and the non-mycorrhizal (NON) treatments started to

Table 2. Parameters for mycorrhizal primary and secondary infection, and growth of external hyphae.

symbol	parameter name	units	value	source
P	probability of primary infection for dispersed inoculum	$cm^{-1}\ d^{-1}$	0.15	assumption
minAge	minimal infection age of a root segment	d	0	assumption
maxAge	maximal infection age of a root segment	d	32	[42]
v_i	rate of internal infection front	$cm\ d^{-1}$	0.13	[36,43]
maxInfection	percentage of maximal infection	—	1	assumption
v	tip elongation rate	$cm\ d^{-1}$	0.13	[25]
a_h	hyphal radius	μm	50	[43]
b	branching rate	d^{-1}	0.5	[25]
hlt	hyphal lifetime	d	10	[25]
θ_h	branching angle	°	60	[44,45]
distTT	threshold for tip–tip anastomosis	cm	0.00	assumption (the value zero deactivates anastomosis)
distTH	threshold for tip–hyphae anastomosis	cm	0.00	assumption (the value zero deactivates anastomosis)
d_e	distance between entry points[a]	cm	0.1	[36,43]
dt	time step for alteration between root growth and infection model	d	1	choice based on root elongation rate

[a]Used for spatial discretization of roots, i.e. $dx = d_e$.

Table 3. Characteristics of the experimental soil used in the sand-soil mixture.

pH (water 1 : 2.5)	7.88
clay (%)	33
silt (%)	24
sand (%)	43
total P ($mg\ kg^{-1}$)	797.00
water extractable P ($mg\ kg^{-1}$)	3.29
total N (%)	0.13
total organic C (%)	2.26

appear at nine weeks from planting ($p > 0.05$) but were only significant at the final harvest 12 weeks from planting ($p < 0.01$; electronic supplementary material, table S1). The initially quite poor plant growth was due to a failure of the inoculated rhizobia to nodulate *M. truncatula*. Following the N fertilization, the rate of plant growth markedly increased. First traces of AM root colonization were visible in individual pots five weeks from planting, whereas significant levels of AM root colonization and external hyphae were only observed at seven weeks after planting and onwards.

For model calibration, we used the data from the AM pots and acknowledged the fact of delayed plant development by reducing the simulation time by 30 days, i.e. simulation time $t = 0$ was set at 30 days after planting.

Root architectural parameters were obtained from image analysis of *M. truncatula* root systems from a different experiment than ours. Out of the 29 root growth parameters, we calibrated four parameters that were not easily accessible in the previous dataset, so that modelled root length fitted the one measured in the validation experiment: the initial elongation rates of the tap root and first-order laterals as well as the maximum number of branches of first-order laterals. The corresponding parameter set was the basis for the further sensitivity analysis.

Owing to the delayed root development in the experiment, the AM development was also delayed so that stage 2 of the experiment did not start with pots that contained a well-established, homogeneous mycelium. Therefore, the starting point for the simulation was not an evenly dispersed inoculum in the pot. AM hyphae extending from the plants in stage 1 did not fill the whole volume of the mesh bags for stage 2, but only penetrated the mesh from each side to grow a certain distance inside the pot, leaving the inner volume of the pots initially with no AM fungal inoculum. We calibrated the penetration distance of hyphae into the mesh containers based on 10 different realizations of the root system, with the best result obtained with a distance of only 0.1 cm. This means that the external hyphae have just barely passed the mesh and almost all of the pot was initially free of the inoculum.

Based on this result, we calculated 100 realizations of the mycorrhizal root system. Figure 2 shows that measured and simulated values of root length, the percentage of root length infected and hyphal length density agree well. This agreement indicates that the most important processes are sufficiently recognized in the model and that the set of model parameters used for the simulations is realistic. Figure 3 visualizes two 21-day-old simulated mycorrhizal root systems under unconfined root growth when inoculum is (*a*) dispersed (*b*) concentrated. Figure 3*a* additionally includes a close-up view of the simulated three-dimensional branching structure of the mycorrhizal root system. The dynamics of root growth and simultaneous infection can be seen in the electronic

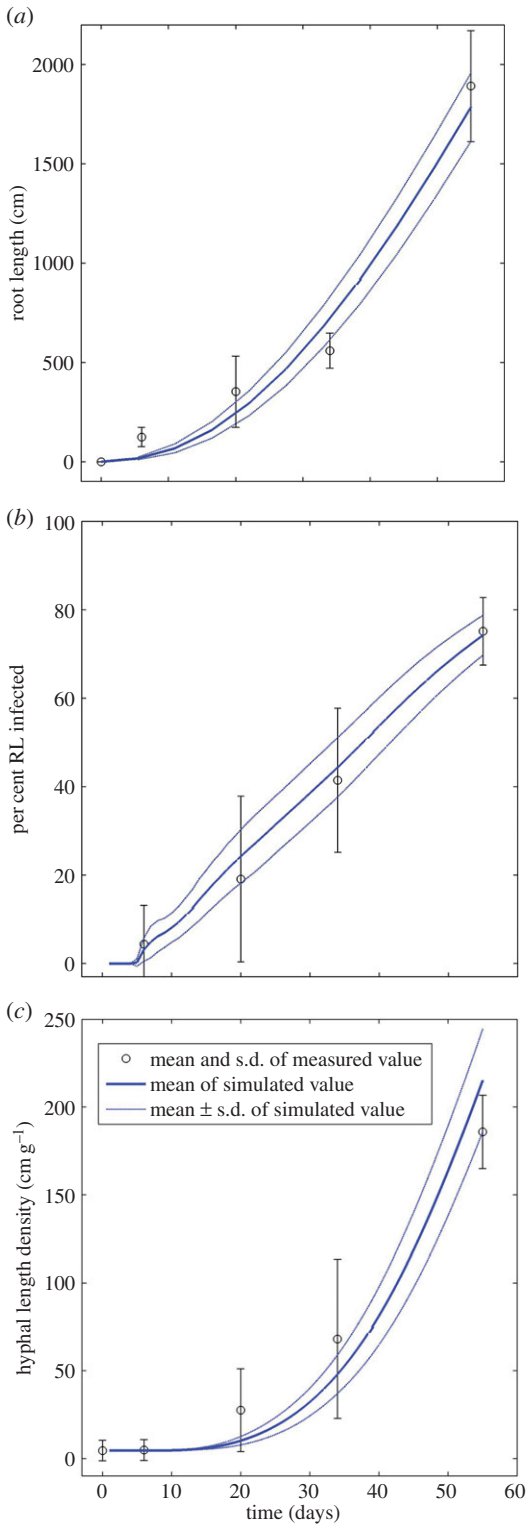

Figure 2. Simulated and measured values of (*a*) root length, (*b*) % root length infected, (*c*) hyphal length density inside the pot after 55 days. The simulation time $t = 0$ was set at 30 days after planting in order to acknowledge delayed plant development. Circles and error bars represent mean and standard deviation of measured data. Solid lines and dotted lines represent mean and standard deviation of simulated data. (Online version in colour.)

supplementary material, S1 and S2, videos of simulation scenarios for dispersed and concentrated inoculum.

6.2. Sensitivity analysis

Sensitivity analysis for four fungal parameters was performed for two scenarios of inoculum position, dispersed and concentrated. All results are based on simulations with a sample size of 100 realizations of a 21-day-old root system.

The standard value of the speed of secondary infection given in table 2 ($v_i = 0.13$ cm d^{-1}) was varied in the range of 0.05 and 1 cm d^{-1} while keeping all other parameters the same. Figure 4 shows the relative change in percentage of infected root length versus the relative change in speed of secondary infection. It can be seen that increasing the speed of secondary infection has a larger effect on root system colonization in the concentrated than in the dispersed case. This is because the speed of secondary infection reaches a value in the order of the root elongation rate or even larger and thus the hyphae could potentially colonize almost the whole root system even when starting from a small zone of concentrated inoculum near the seed. In the dispersed case, any root segment can become infected at any time. Here, increasing the speed of secondary infection also increases the percentage of infected root length, but quickly reaches the maximal infection.

Sensitivity analysis regarding branching rate (b), distance between entry points (dx), and *hlt* was again performed by varying one parameter at a time while leaving the others the same. The standard value of b given in table 2 ($b = 0.5$) was varied in the range of 0.1–10 d^{-1}, standard value of dx (d$x = 0.1$ cm) in the range of 0.02–10 cm and the standard value of *hlt* (*hlt* = 6) in the range of 4–10 days. This time, the effect on simulated hyphal length density was assessed.

Figure 5*a* shows the relative change in hyphal length density owing to varying the hyphal lifetime. Hyphal length density increases with increasing hyphal lifetime for both dispersed and placed inoculum. However, the effect is much stronger in case of concentrated inoculum. Doubling the hyphal lifetime leads to a fivefold increase in the realized hyphal length density. This is due to the fact that more external hyphae are initiated earlier when the inoculum is concentrated near the seed while in the dispersed case there are more younger and still less elongated hyphae at any time of development and thus considering a greater lifespan does not have such a high impact.

Figure 5*b* shows the relative change in hyphal length density owing to varying the hyphal branching rate. Although the absolute values are different in the dispersed and concentrated cases, the relative change is independent of the inoculum position. Increasing the hyphal branching rate increases hyphal length density, and doubling it already results in a fourfold increase in hyphal length density.

Figure 5*c* shows the relative change in hyphal length density owing to varying the distance between entry points. Increasing the distance between entry points, which would reflect a lower propagule density, results in a decrease of hyphal length density, and the relative effect is again independent of the inoculum position.

7. Discussion

7.1. Model development

We extended an L-system model for root architecture to include root infection with AM fungi and growth of their hyphae in soil. In terms of previous model classification [19], it is a lattice-free model where the mycelial network is not constrained to a predetermined grid or lattice. Our model is similar to previous approaches for other filamentous

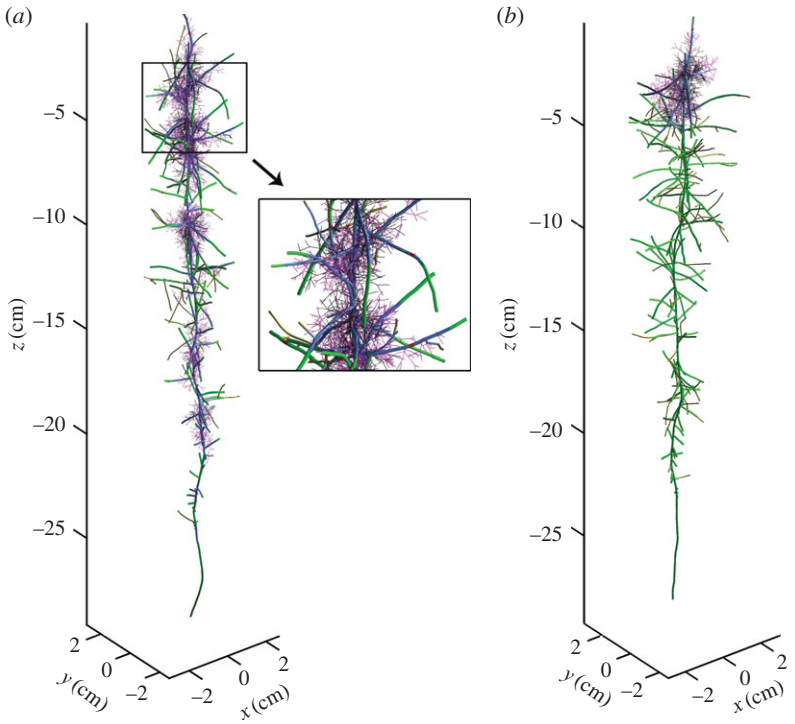

Figure 3. Twenty-one day old simulated mycorrhizal root system with unconfined root growth and (*a*) dispersed inoculum with infection probability 0.15; close-up of part of the mycorrhizal root (*b*) concentrated inoculum with infection probability 1. Green, uninfected root segment; red, root segment infected by primary infection; blue, root segment infected by secondary infection; magenta, external hyphae up to 10 days old; black, dead roots or external hyphae.

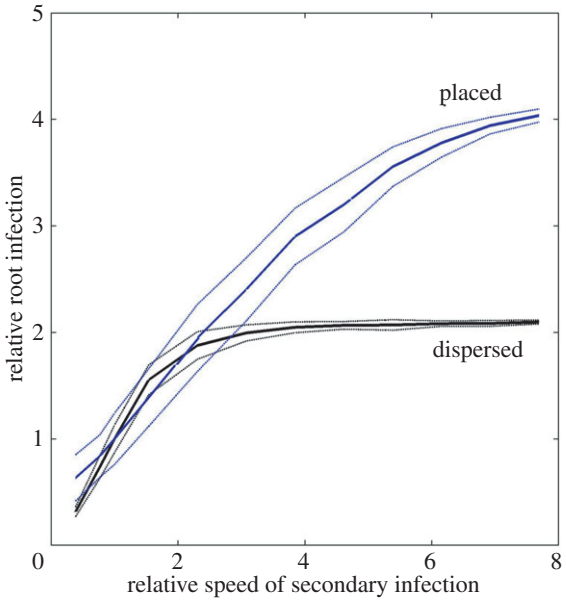

Figure 4. Change in relative % of root length infected owing to varying the speed of secondary infection compared with the standard value ($v_i = 0.13$). Two cases of inoculum are considered, concentrated (results shown in blue) and dispersed (results shown in black). Solid and dotted lines represent mean and standard deviation of 100 realizations of a 21-day-old root system.

fungi [50,51] regarding that the fungal network (like the root system) is represented by a collection of line segments as well as tips that can extend with time. At each time step, there is the possibility of hyphal fusion, and a reorientation of the direction of growth. Although it was deactivated in the simulations presented here, we know from earlier work, [25,26], that the effect of anastomosis is twofold. First, it reduces the number of hyphal tips and thus production of new hyphal segments. Second, it creates an interconnected network which will impact flow and transport of e.g. carbon or phosphate inside the mycelium. In a future work, we will explore this further, as well as the effects of different types of tropisms on the spatial distribution of hyphae in soil, including negative autotropism (measured with respect to the density of other line segments), galvanotropism (based on self-generated electric fields that either align or diverge in respect to adjacent hyphae) and gravitropism (with growth either following or opposing the gravitational field), but also soil-dependent tropisms such as chemotropism or hydrotropism.

7.2. Model predictions

The model predicts the three-dimensional root and hyphal architecture for different placements of inoculum. These are the first model results that dynamically follow the infection within the root system in a spatially resolved way. As such, this model offers a very useful framework for optimization of inoculum placement to achieve a predefined rate of root system infection, provided the patterns of root and soil colonization for a given AM fungal taxon are known [7]. Further, the model provides some mechanistic explanation of how a maximum level of root colonization is achieved (frequently reported in the literature [36]), taking into account the growth rates of both root and the AM fungal hyphae. A 100% infection rate would only be possible when the density of inoculum is very high or the secondary infection fronts advance faster than root growth. The overall infection is thus dependent on the infectivity and position of the inoculum and the speed of secondary infection. A user-defined smaller value for a maximal infection would result in the fact that further infection is determined by the rate of root system growth once the maximal infection is reached. When

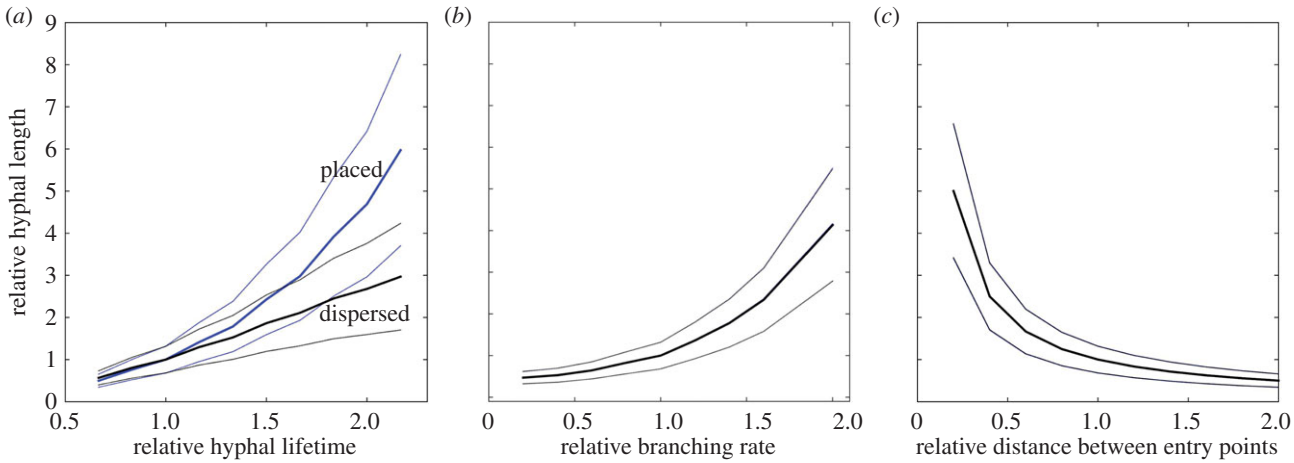

Figure 5. Sensitivity analysis of fungal growth parameters. (*a*) Relative change in hyphal length owing to varying the hyphal lifetime (standard value $htl = 6$ d). (*b*) Relative change in hyphal length due to varying the branching rate (standard value $b = 0.5\ \mathrm{d}^{-1}$). (*c*) Relative change in hyphal length owing to varying the distance between entry points (standard value $d_e = 0.1$ cm). Two variants of inoculum placement are considered, concentrated (results shown in blue) and dispersed (results shown in black). Results for both scenarios overlap in (*b*) and (*c*) and thus only one is shown. Solid and dotted lines represent mean and standard deviations of 100 realizations of a 21-day-old root system.

secondary infection is fast, the differences between inoculum positions are only significant in the initial phase of colonization. When inoculum is placed near the seed, roots become immediately infected. However, when inoculum is dispersed in soil, there is a time lag until first infections are visible.

7.3. Model limitations

Our model includes both root and hyphal death. However, we still recommend using it only for simulating young root systems, as for the older ones, important processes might still be missing.

The interaction between the mycorrhizal root system and soil, such as carbon flow into the soil and external hyphae from roots [52–55], needs to be considered. Currently, the model does also not account for autoregulation of mycorrhization [56,57], where further root colonization by AM fungi in already mycorrhizal plants may be suppressed after a critical level of root colonization is achieved.

The model could be extended to include morphogenetic changes to root systems through mycorrhization [58], and also to account for different morphogenetic structures of external fungal hyphae [44]. Like most fungal growth models, it currently assumes the hyphae being a network of homogeneous structures [19], i.e. it ignores structural and functional differentiation within the external hyphae networks that might be functionally important [44]. A future version of the model might distinguish between runner hyphae, likely to be mainly responsible for secondary infection, and branched absorbing structures, likely to be mainly involved in soil exploitation. At this point in time our focus was to show how root architecture and topology as well as inoculum position in soil influence the internal colonization of a growing root system.

7.4. Modelling outlook

We are keen to extend our model to include external mycelial structure in our future work supported by suitable experimental data. Importantly, model validation has so far been carried out only for single-species systems, so it will need to be parametrized for different AM fungal and plant taxa, and eventually for their mixtures to achieve a greater ecosystem relevancy. It also does not take into account possible soil heterogeneity, which may induce feedback on both the root and hyphae growth [59]. The model should ultimately allow disentangling the feedback between mycorrhiza development and matter (nutrient, water and carbon) fluxes between soil, mycorrhiza and plants. It seems we successfully achieved the first steps, the others need to follow. To this end, data on P acquisition of the mycorrhizal plants from the validation experiment described above will serve in a follow-up work when the mycorrhiza model will be linked to a soil model as approached previously on the single root scale [26]. Including carbon flow will be of great interest to study and compare the carbon costs of different plant mechanisms for increasing uptake of P, i.e. mycorrhiza versus root hairs [60], and mycorrhiza versus root exudation [61].

Authors' contributions. A.S., D.L., P.F.S. and J.J. designed the research; P.F.S. and J.J. designed the validation experiment; P.F.S. and P.S. performed the validation experiment; J.J. performed the real-time PCR analysis; D.L. and A.S. undertook model development and Matlab implementation; P.S. participated in data analysis; A.S. coordinated the study and mainly drafted the manuscript; D.L., J.J., P.F.S. and P.S. helped draft the manuscript. All authors gave final approval for publication.

Data accessibility. All data are provided in the electronic supplementary material. These include the images of *M. truncatula* along with the Matlab workspace after image analysis with RootSystemAnalyzer (electronic supplementary material, S3), the results of the validation experiment (electronic supplementary material, S4) and the Matlab m-files that extend the RootBox model to simulate mycorrhization (electronic supplementary material, S5).

Competing interests. We declare to have no competing interests.

Funding. A.S., P.F.S. and P.S. were partly supported by the Austrian Science Fund FWF (grant no.: T341-N13). J.J. was supported by Fellowship J. E. Purkyně, Czech Ministry of Education, Youth and Sports (LK11224), and the long-term development programme RVO61388971, D.L. is recipient of an APART-fellowship of the Austrian Academy of Sciences at the Computational Science Center, University of Vienna.

Acknowledgements. We thank Marie-Theres Hauser for providing microscopy facilities, Virginie Bourion for providing images of scanned *M. truncatula* root systems, INRA Toulouse for providing *S. meliloti* strain, and Willibald Loiskandl for discussions and suggestions.

References

1. Wyatt GAK, Kiers ET, Gardner A, West SA. 2014 A biological market analysis of the plant–mycorrhizal symbiosis. *Evolution* **68**, 2603–2618. (doi:10.1111/evo.12466)
2. Treseder K. 2013 The extent of mycorrhizal colonization of roots and its influence on plant growth and phosphorus content. *Plant Soil* **371**, 1–13. (doi:10.1007/s11104-013-1681-5)
3. Jakobsen I, Abbott LK, Robson AD. 1992 External hyphae of vesicular-arbuscular mycorrhizal fungi associated with *Trifolium subterraneum* L. *New Phytol.* **120**, 371–380. (doi:10.1111/j.1469-8137.1992.tb01077.x)
4. Munkvold L, Kjøller R, Vestberg M, Rosendahl S, Jakobsen I. 2004 High functional diversity within species of arbuscular mycorrhizal fungi. *New Phytol.* **164**, 357–364. (doi:10.1111/j.1469-8137.2004.01169.x)
5. Jansa J, Smith FA, Smith SE. 2008 Are there benefits of simultaneous root colonization by different arbuscular mycorrhizal fungi? *New Phytol.* **177**, 779–789. (doi:10.1111/j.1469-8137.2007.02294.x)
6. Lendenmann M, Thonar C, Barnard RL, Salmon Y, Werner RA, Frossard E, Jansa J. 2011 Symbiont identity matters: carbon and phosphorus fluxes between *Medicago truncatula* and different arbuscular mycorrhizal fungi. *Mycorrhiza* **21**, 689–702. (doi:10.1007/s00572-011-0371-5)
7. Thonar C, Schnepf A, Frossard E, Roose T, Jansa J. 2011 Traits related to differences in function among three arbuscular mycorrhizal fungi. *Plant Soil* **339**, 231–245. (doi:10.1007/s11104-010-0571-3)
8. Duke SE, Jackson RB, Caldwell MM. 1994 Local reduction of mycorrhizal arbuscule frequency in enriched soil microsites. *Can. J. Bot.* **72**, 998–1001. (doi:10.1139/b94-125)
9. Treseder KK, Allen MF. 2002 Direct nitrogen and phosphorus limitation of arbuscular mycorrhizal fungi: a model and field test. *New Phytol.* **155**, 507–515. (doi:10.1046/j.1469-8137.2002.00470.x)
10. Schroeder MS, Janos DP. 2005 Plant growth, phosphorus nutrition, and root morphological responses to arbuscular mycorrhizas, phosphorus fertilization, and intraspecific density. *Mycorrhiza* **15**, 203–216. (doi:10.1007/s00572-004-0324-3)
11. Genre A, Chabaud M, Faccio A, Barker DG, Bonfante P. 2008 Prepenetration apparatus assembly precedes and predicts the colonization patterns of arbuscular mycorrhizal fungi within the root cortex of both *Medicago truncatula* and *Daucus carota*. *Plant Cell* **20**, 1407–1420. (doi:10.1105/tpc.108.059014)
12. Friese C, Allen M. 1991 The spread of VA mycorrhizal fungal hyphae in the soil: inoculum types and external hyphal architecture. *Mycologia* **83**, 409–418. (doi:10.2307/3760351)
13. VanDer Heijden MGA, Scheublin TR. 2007 Functional traits in mycorrhizal ecology: their use for predicting the impact of arbuscular mycorrhizal fungal communities on plant growth and ecosystem functioning. *New Phytol.* **174**, 244–250. (doi:10.1111/j.1469-8137.2007.02041.x)
14. Buwalda JG, Stribley DP, Tinker PB. 1984 The development of endomycorrhizal root systems. V. The detailed patterns of development of infection and the control of infection level by host in young leek plants. *New Phytol.* **96**, 411–427. (doi:10.1111/j.1469-8137.1984.tb03576.x)
15. Bruce A, Smith SE, Tester M. 1994 The development of mycorrhizal infection in cucumber: effects of P supply on root growth, formation of entry points and growth of infection units. *New Phytol.* **127**, 507–514. (doi:10.1111/j.1469-8137.1994.tb03968.x)
16. Rosling A, Roose T, Herrmann AM, Davidson FA, Finlay RD, Gadd GM. 2009 Approaches to modelling mineral weathering by fungi. *Fungal Biol. Rev.* **23**, 138–144. (doi:10.1016/j.fbr.2009.09.003)
17. Hopkins S, Boswell GP. 2012 Mycelial response to spatiotemporal nutrient heterogeneity: a velocity-jump mathematical model. *Fungal Ecol.* **5**, 124–136. (doi:10.1016/j.funeco.2011.06.006)
18. Cunniffe NJ, Gilligan CA. 2008 Scaling from mycelial growth to infection dynamics: a reaction diffusion approach. *Fungal Ecol.* **1**, 133–142. (doi:10.1016/j.funeco.2008.10.007)
19. Boswell GP, Davidson FA. 2012 Modelling hyphal networks. *Fungal Biol. Rev.* **26**, 30–38. (doi:10.1016/j.fbr.2012.02.002)
20. McGonigle TB. 2001 On the use of non-linear regression with the logistic equation for changes with time of percentage root length colonized by arbuscular mycorrhizal fungi. *Mycorrhiza* **10**, 249–254. (doi:10.1007/s005720000080)
21. Bever JD. 2015 Preferential allocation, physio-evolutionary feedbacks, and the stability and environmental patterns of mutualism between plants and their root symbionts. *New Phytol.* **205**, 1503–1514. (doi:10.1111/nph.13239)
22. Landis FC, Fraser LH. 2008 A new model of carbon and phosphorus transfers in arbuscular mycorrhizas. *New Phytol.* **177**, 466–479.
23. Buwalda JG, Ross GJS, Stribley DP, Tinker PB. 1982 The development of endomycorrhizal root systems. III. The mathematical representation of the spread of vesicular–arbuscular mycorrhizal infection in root systems. *New Phytol.* **91**, 669–682. (doi:10.1111/j.1469-8137.1982.tb03346.x)
24. Buwalda JG, Ross GJS, Stribley DP, Tinker PB. 1982 The development of endomycorrhizal root systems. IV. The mathematical analysis of effects of phosphorus on the spread of vesicular–arbuscular mycorrhizal infection in root systems. *New Phytol.* **92**, 391–399. (doi:10.1111/j.1469-8137.1982.tb03396.x)
25. Schnepf A, Roose T, Schweiger P. 2008 Growth model for arbuscular mycorrhizal fungi. *J. R. Soc. Interface* **5**, 773–784. (doi:10.1098/rsif.2007.1250)
26. Schnepf A, Roose T, Schweiger P. 2008 Impact of growth and uptake patterns of arbuscular mycorrhizal fungi on plant phosphorus uptake—a modelling study. *Plant Soil* **312**, 85–99. (doi:10.1007/s11104-008-9749-3)
27. Leitner D, Klepsch S, Bodner G, Schnepf A. 2010 A dynamic root system growth model based on L-systems. *Plant Soil* **332**, 177–192. (doi:10.1007/s11104-010-0284-7)
28. Leitner D, Klepsch S, Knieß A, Schnepf A. 2010 The algorithmic beauty of plant roots—an L-system model for dynamic root growth simulation. *Math. Comput. Model. Dyn. Syst.* **16**, 575–587. (doi:10.1080/13873954.2010.491360)
29. Hart MM, Reader RJ. 2002 Taxonomic basis for variation in the colonization strategy of arbuscular mycorrhizal fungi. *New Phytol.* **153**, 335–344. (doi:10.1046/j.0028-646X.2001.00312.x)
30. Sanders FE, Tinker PB, Black RLB, Palmerley SM. 1977 The development of endymycorrhizal root systems: I. Spread of infection and growth-promoting effects with four species of vesicular-arbuscular endophyte. *New Phytol.* **78**, 257–268. (doi:10.1111/j.1469-8137.1977.tb04829.x)
31. Smith SE, Walker NA. 1981 A quantitative study of mycorrhizal infection in *Trifolium*: separate determination of the rates of infection and of mycelial growth. *New Phytol.* **89**, 225–240. (doi:10.1111/j.1469-8137.1981.tb07485.x)
32. Jakobsen I, Abbott LK, Robson AD. 1992 External hyphae of vesicular-arbuscular mycorrhizal fungi associated with *Trifolium subterraneum* L. 2. Hyphal transport of ^{32}P over defined distances. *New Phytol.* **120**, 509–516. (doi:10.1111/j.1469-8137.1992.tb01800.x)
33. Black R, Tinker PB. 1979 The development of endymycorrhizal root systems. II. Effect of agronomic factors and soil conditions on the development of vesicular-arbuscular mycorrhizal infection in barley and on the endophyte spore density. *New Phytol.* **83**, 401–413. (doi:10.1111/j.1469-8137.1979.tb07465.x)
34. Amijee F, Stribley DP, Tinker PB. 1986 The development of endomycorrhizal root systems. VI. The relationship between development of infection, and intensity of infection in young leak roots. *New Phytol.* **102**, 293–301. (doi:10.1111/j.1469-8137.1986.tb00584.x)
35. Amijee F, Tinker PB, Stribley DP. 1989 The development of endomycorrhizal root systems. VII. A detailed study of effects of soil phosphorus on colonization. *New Phytol.* **111**, 435–446. (doi:10.1111/j.1469-8137.1989.tb00706.x)
36. Amijee F, Stribley DP, Tinker PB. 1993 The development of endomycorrhizal root systems. VIII. Effects of soil phosphorus and fungal colonization on the concentration of soluble carbohydrates in roots. *New Phytol.* **123**, 1469–8137. (doi:10.1111/j.1469-8137.1993.tb03739.x)
37. Abbott LK, Robson AD, Jasper DA, Gazey C. 1992 What is the role of VA mycorrhizal hyphae in soil? In

Mycorrhizas in ecosystems, Wallingford, UK: CAB International.

38. Sanders FE, Sheikh NA. 1983 The development of vesicular–arbuscular mycorrhizal infection in plant root systems. *Plant Soil* **71**, 223–246. (doi:10.1007/BF02182658)
39. Bourion V *et al.* 2014 Unexpectedly low nitrogen acquisition and absence of root architecture adaptation to nitrate supply in a *Medicago truncatula* highly branched root mutant. *J. Exp. Bot.* **65**, 2365–2380. (doi:10.1093/jxb/eru124)
40. Leitner D, Felderer B, Vontobel P, Schnepf A. 2014 Recovering root system traits using image analysis exemplified by two-dimensional neutron radiography images of lupine. *Plant Physiol.* **164**, 24–35. (doi:10.1104/pp.113.227892)
41. Dunbabin VM *et al.* 2013 Modelling root–soil interactions using three-dimensional models of root growth, architecture and function. *Plant Soil* **372**, 93–124. (doi:10.1007/s11104-013-1769-y)
42. Hepper CM. 1985 Influence of age of roots on the pattern of vesicular–arbuscular mycorrhizal infection in leek and clover. *New Phytol.* **101**, 685–693. (doi:10.1111/j.1469-8137.1985.tb02874.x)
43. Ezawa T, Smith SE, Smith FA. 2002 P metabolism and transport in AM fungi. *Plant Soil* **244**, 221–230. (doi:10.1023/A:1020258325010)
44. Bago B, Azcón-Aguilar C, Goulet A, Piché Y. 1998 Branched absorbing structures (BAS): a feature of the extraradical mycelium of symbiotic arbuscular mycorrhizal fungi. *New Phytol.* **139**, 375–388. (doi:10.1046/j.1469-8137.1998.00199.x)
45. Bago B, Cano C, Azcón-Aguilar C, Samson J, Coughlan AP, Piché Y. 2004 Differential morphogenesis of the extraradical mycelium of an arbuscular mycorrhizal fungus grown monoxenically on spatially heterogeneous culture media. *Mycologia* **96**, 452–462. (doi:10.2307/3762165)
46. McGonigle TP, Miller MH, Evans DG, Fairchild GL, Swan JA. 1990 A new method which gives an objective measure of colonization of roots by vesicular–arbuscular mycorrhizal fungi. *New Phytol.* **115**, 495–501. (doi:10.1111/j.1469-8137.1990.tb00476.x)
47. Vierheilig H, Schweiger P, Brundrett M. 2005 An overview of methods for the detection and observation of arbuscular mycorrhizal fungi in roots. *Physiol. Plant.* **125**, 393–404. (doi:10.1111/j.1399-3054.2005.00564.x)
48. Thonar C, Erb A, Jansa J. 2012 Real-time PCR to quantify composition of arbuscular mycorrhizal fungal communities—marker design, verification, calibration and field validation. *Mol. Ecol. Resour.* **12**, 219–232. (doi:10.1111/j.1755-0998.2011.03086.x)
49. Jansa J, Erb A, Oberholzer H-R, Šmilauer P, Egli S. 2014 Soil and geography are more important determinants of indigenous arbuscular mycorrhizal communities than management practices in Swiss agricultural soils. *Mol. Ecol.* **23**, 2118–2135. (doi:10.1111/mec.12706)
50. Carver I, Boswell GP. 2008 A lattice-free model of translocation-induced outgrowth in fungal mycelia. *IAENG Int. J. Appl. Math.* **38**, 173–179.
51. Meškauskas A, McNulty LJ, Moore D. 2004 Concerted regulation of all hyphal tips generates fungal fruit body structures: experiments with computer visualizations produced by a new mathematical model of hyphal growth. *Mycol. Res.* **108**, 341–353. (doi:10.1017/S0953756204009670)
52. Snellgrove RC, Splittstoesser WE, Stribley DP, Tinker PB. 1982 The distribution of carbon and the demand of the fungal symbiont in leek plants with vesicular–arbuscular mycorrhizas. *New Phytol.* **92**, 75–87. (doi:10.1111/j.1469-8137.1982.tb03364.x)
53. Jakobsen I, Rosendahl L. 1990 Carbon flow into soil and external hyphae from roots of mycorrhizal cucumber plants. *New Phytol.* **115**, 77–83. (doi:10.1111/j.1469-8137.1990.tb00924.x)
54. Schwab SM, Menge JA, Tinker PB. 1991 Regulation of nutrient transfer between host and fungus in vesicular–arbuscular mycorrhizas. *New Phytol.* **117**, 387–398. (doi:10.1111/j.1469-8137.1991.tb00002.x)
55. Jones DL, Hodge A, Kuzyakov Y. 2004 Plant and mycorrhizal regulation of rhizodeposition. *New Phytol.* **163**, 459–480. (doi:10.1111/j.1469-8137.2004.01130.x)
56. Vierheilig H. 2004 Further root colonization by arbuscular mycorrhizal fungi in already mycorrhizal plants is suppressed after a critical level of root colonization. *J. Plant Physiol.* **161**, 339–341. (doi:10.1078/0176-1617-01097)
57. Vierheilig H. 2004 Regulatory mechanisms during the plant–arbuscular mycorrhizal fungus interaction. *Can. J. Bot.* **82**, 1166–1176. (doi:10.1139/B04-015)
58. Berta G, Fusconi A, Trotta A, Scannerini S. 1990 Morphogenetic modifications induced by the mycorrhizal fungus *Glomus* strain E3 in the root system of *Allium porrum* L. *New Phytol.* **114**, 207–215. (doi:10.1111/j.1469-8137.1990.tb00392.x)
59. Felderer B, Jansa J, Schulin R. 2013 Interaction between root growth allocation and mycorrhizal fungi in soil with patchy P distribution. *Plant Soil* **373**, 569–582. (doi:10.1007/s11104-013-1818-6)
60. Jakobsen I, Chen B, Munkvold L, Lundsgaard T, Zhu Y-G. 2005 Contrasting phosphate acquisition of mycorrhizal fungi with that of root hairs using the root hairless barley mutant. *Plant Cell Environ.* **28**, 928–938. (doi:10.1111/j.1365-3040.2005.01345.x)
61. Kaiser C, Kilburn MR, Clode PL, Fuchslueger L, Koranda M, Cliff JB, Solaiman ZM, Murphy DV. 2015 Exploring the transfer of recent plant photosynthates to soil microbes: mycorrhizal pathway vs direct root exudation. *New Phytol.* **205**, 1537–1551. (doi:10.1111/nph.13138)